Research on Recognition of Polynyas Based on AMSR2 Data of Microwave Radiometer

Haowei Zhang, Xingdong Wang, Huilin Niu

College of Information Science and Engineering, Henan University of Technology, Zhengzhou, 450001 Henan, China

Abstract: The polynyas is formed under the combined action of ocean, atmosphere and sea ice. It is closely related to ice conditions, dynamic and thermal processes in water bodies, and atmospheric circulation, and plays an important role in the climate system. This paper proposes a new method for detecting the distribution of polynyas based on AMSR2 19GHz data. First, the 19GHz vertical and horizontal brightness temperature data are processed to obtain the polarization difference. Secondly, the maximum entropy method is used to process the polarization difference data to obtain the optimal threshold for the identification of the polynyas, so as to obtain the results of the polynyas on October 15, 2017. Finally, the method proposed in this paper is comparing with the sea ice density threshold method. The results show that the distribution results of polynyas obtained by the two are basically the same, and its accuracy is higher than that of the sea ice density threshold method.

Keywords: polynyas, polarization, difference, AMSR2

1. Introduction

The polynyas is the water area that appears in the sea ice area without ice or only covered by thin ice under the weather condition that the sea ice is frozen[1]. The traditional classification of interglacial lakes is mainly divided into two categories (sensible heat polynyas and latent heat polynyas) according to their formation reasons and maintenance mechanisms[2]. The sensible heat polynyas is mainly driven by heat. The warm deep ocean water rises under the action of convective mixing, allowing heat to enter the surface layer to melt the sea ice and prevent the formation of new ice, forming an interglacial lake inside the sea ice covered area. The latent heat polynyas is mainly driven by power. It is mainly driven by wind or ocean currents. Because the water temperature in the interglacial lake is close to the freezing point and heat is lost through the sea-air interface, a large amount of new ice is formed, and the newly formed sea ice is in the wind or ocean currents. Divergence occurs under the action of, resulting in open water. The heat flux exchange between the atmosphere-ice-ocean in the polynyas is much larger than that of other thick ice regions, and it is the main ice producing area[3]. The polynyas plays an important role in climate change. The ocean-atmosphere heat exchange in its interior is very significant, which can lead to rapid air temperature increase in the upper and lower winds, and therefore has an important impact on the local atmospheric circulation[4]. In recent years, there have been many studies related to polynyas. Liang et al. used AMSR-E daily average sea ice density data to count the frequency of occurrence of polynyas along the Alaska coast of the Chukchi Sea, at the same time, combined with the NCEP-DOE analysis of wind field data and the temperature and salinity and ocean current data of the Bering Strait submarine standard observations, the occurrence and development of polynyas are discussed[5]. Fu et al. studied the seasonal and interannual changes in the area of clean water, net heat flux, ice production and salt production in the Arctic polynyas, and compared the differences between different polynyas[6]. Massom et al. proposed that the 75% density threshold should be used to extract and identify polynyas. The basis for the judgment is that the sea ice density is between 0% and 75% as the polynyas, and the sea ice density is between 75% and 100%. Between sea ice[7]. Stringer et al. used visible light satellite images (AVHRR, Advanced Very High Resolution Radiometer) to analyze the polynyas in the Bering Sea and the Chukchi Sea shelf area, and obtained high-resolution information of the glacial lakes. However, the polynyas are usually cloudy and foggy, with visible light. And the infrared image is interfered by it, and the continuity of observation cannot be guaranteed[8]. Ciappa et al. used the ice surface temperature map retrieved from MODIS thermal infrared band images to extract the range of Terra Nova Bay polynyas under clear skies, and processed several thousand images from 2005 to 2010. Due to the surface temperature Affected by temperature, each image uses a different ice temperature threshold, but all thresholds are below the sea ice point of 271.5K[9]. Haid et al. used 70% density and sea ice thickness of 20 cm as the threshold to extract the coastal polynyas in the southwest of the Weddell Sea[10]. For the extraction and identification of ice lakes, currently most of the threshold methods based on sea ice density are used. The accuracy of the sea ice density result obtained by the sea ice density inversion algorithm is not high (in the low ice density area, the uncertainty of the sea ice density result is as high as 25%[11], in the edge ice area, the sea ice density result is The results of comparison with SAR and optical images show that the root mean square error is as high as 26.2%[12]), which is

used as the data basis for identifying polynyas, which will inevitably lead to larger errors in the identification results of polynyas.

In order to improve the recognition accuracy of the polynyas, this paper proposes a new method of combining polarization difference and maximum entropy to identify lakes between ice, that is, processing AMSR2 19GHz polarization difference data by the maximum entropy method to obtain the optimal threshold for recognition of polynyas, then obtain the distribution of polynyas, and Contrast verification with the sea ice density threshold method.

2. Research Area and Data Source

2.1 Research area

The polynyas studied in this article is located in the Hakon VII Sea, and it is named to commemorate the first king of Norway, Haakon VII after the disintegration of Sweden. The sea area is located between the Weddell Sea and the Lazarev Sea. The central area extends from the Cape of Norway along the coast of Princess Marta to the Fibre Ice Shelf, close to the Prime Meridian. The approximate coordinates of the sea area are 20 ℃W ~45 ℃E, with a total length of about 6,270 miles, and are covered by ice for most of the year.

2.2 Data source

This article uses AMSR2 sensor data for analysis and research, which is mounted on the Earth's water environment change monitoring satellite "GCOM-W1", launched by the Japan Aerospace Exploration Agency (JAXA) on May 8, 2012, which can provide the Earth's water and energy cycle Long-term monitoring data. It inherits all frequency channels of AMSR-E, and adds 2 channels with a frequency of 7.3GHz, so as to prevent the observation data from RFI (Radio Frequency Interference) interference in terrestrial areas as much as possible. AMSR2 is a conical scanning sensor with a scanning angle of 47.5 °, and a single scan can cover a width of 1450km on the ground. Compared with the previous version AMSR-E (scanning angle of 47.4 °, scanning width of 1445km), it has improved. Observation data obtained in two days can cover more than 99% of the world. AMSR2 provides daily and monthly average ECP grid data products with a resolution of 0.1 ℃0.25 °(10/25km).

3. Research Method

3.1 Polarization difference

The spectral characteristics of ground features are the basis of remote sensing inversion. The spectral characteristic curves of different ground features reflect the difference in electromagnetic wave reflection of different ground features. Among them, the spectral characteristic curves of sea water and sea ice are shown in Figure 1. According to the definition of brightness temperature, when the physical temperature of an object is constant, the brightness temperature at a certain frequency is only related to the emissivity of the object. Because when vertically polarized and horizontally polarized electromagnetic waves are emitted simultaneously on the surface of sea water or sea ice, the physical temperature of the same object is the same, so the polarization difference is only affected by the emissivity. From the results in Figure 1, it can be seen that in these frequency bands of AMSR2, the polarization difference of sea water at 19 GHz differs the most from sea ice. The polarization difference of 19 GHz P = 19V －19H can be used to identify the difference between sea water and sea ice. The sea ice then gets the distribution of the polynyas. That is, if P > Th, then this pixel is an polynya, otherwise it is sea ice.

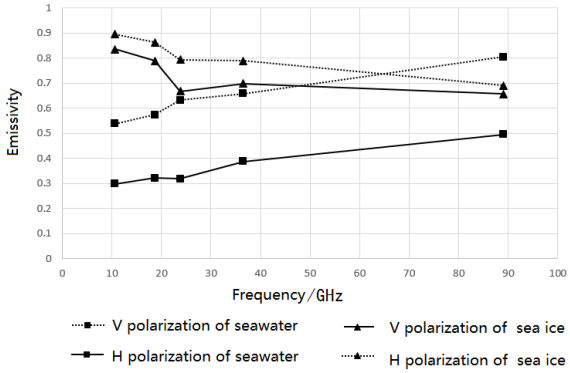

Figure 1. Relationship between emissivity and frequency of sea water and sea ice

3.2 Maximum entropy method

The maximum entropy method is based on the "information entropy" proposed by Claude Elwood Shannon in 1948. The principle is as follows:

According to the definition of entropy in information theory, after a given image, the entropy of the image can already be calculated according to equation (1).

$$H = -\int_{-\infty}^{+\infty} p(x)\log[p(x)]dx \qquad (1)$$

Where $p(x)$ represents the frequency of gray x, H represents information entropy.

Select a threshold T to perform image segmentation. All pixels are divided into two categories. Pixels below the threshold T are the background, denoted as B, and pixels higher than the threshold T are the objects, denoted as O.

Calculate the probability of each gray level in the B or O category. The calculation based on the background is shown in equation (2), the calculation based on the object is shown in equation (3), and the relationship between the two is shown in equation (4).

$$\frac{p_i}{p_t}, i = 1, 2, ..., T \qquad (2)$$

$$\frac{p_i}{1 - p_T}, i = T + 1, T + 2, ..., L \qquad (3)$$

$$p_T = \sum_{i=0}^{T} p(i) \qquad (4)$$

Calculate the information entropy of the background and the object respectively, and then obtain the range of the *B* and *O* types as shown in formula (5) and formula (6).

$$H_B = -\sum_i \frac{p_i}{p_T} \log[\frac{p_i}{p_T}] \quad i = 1, 2T, \quad (5)$$

$$H_O = \sum_i \frac{p_i}{1-p_T} \log[\frac{p_i}{1-p_T}], i = T+1, T+2, ..., 2T \quad (6)$$

When each gray level in the image is processed, the optimal segmentation threshold *T* satisfies the following conditions, as shown in equation (7):

$$T = \arg\max(H_B + H_O) \quad (7)$$

3.3 Polarization difference combined with maximum entropy method to identify glacial lakes

The maximum entropy method is used to process the 19 GHz polarization difference P, and the classification threshold Th=49.03 of the polynyas and sea ice is obtained, and then the image is classified to obtain the distribution of the polynyas. Figure 2 is a flow chart of ice lake identification. The basic steps are as follows:

(1) Data preprocessing: radiation calibration, mask, and abnormal data point processing.

(2) Calculate the polarization difference: use the vertical polarization brightness temperature and horizontal polarization brightness temperature of 19 GHz to calculate the polarization difference P=19V-19H.

(3) Determine the optimal threshold for classification of polynyas and sea ice: select the sample area and apply the maximum entropy method to process the polarization difference image to obtain the optimal threshold Th.

(4) Obtain the recognition result of the polynyas: classify the polarization difference image according to the optimal threshold Th, and obtain the recognition result of the polynyas.

(5) Verification: the results obtained are compared and verified with the results based on the sea ice density threshold method.

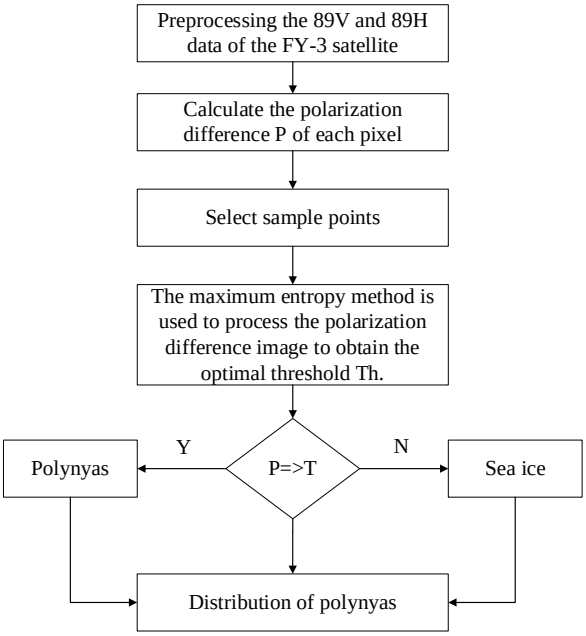

Figure 2. The identification process of the polynyas based on 19GHz data

4. Results

Based on the Hakon VII Sea AMSR2 19GHz horizontal polarization brightness temperature data and vertical polarization brightness temperature data on October 15, 2017, the polarization difference combined with the maximum entropy method to obtain the distribution results of the polynyas as shown in Figure 3, and the distribution result of the polynyas obtained by the threshold method (threshold value is 0.75) as shown in Figure 4. In Figure 3, the total area of the polynyas is about 23700 million km2, and in Figure 4, the total area of the polynyas is about 282.3 million km2. From Figure 3 and Figure 4, it can be seen that the size and distribution of the polynyas are not much different, but the distribution of some marginal areas are different. In Figure 3, the distribution of the polynyas in the red circle does not show many scattered points, while the distribution of the polynyas in the green circle shows a natural disorder, twists and turns. In Figure 4, the distribution of polynyas in the red circle shows the scattered distribution of many individual freezing points, while the distribution of polynyas in the green circle shows a geometrically ordered state. From the above comparison, it can be seen that the polynyas identification method based on the polarization difference combined with the maximum entropy method is effective and feasible. According to the distribution information of the polynyas, it can be explained to a certain extent that the polynyas identification method proposed in this paper has higher accuracy.

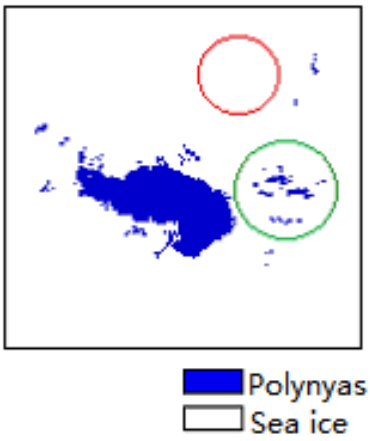

Figure 3. Polarization difference combined with maximum entropy method

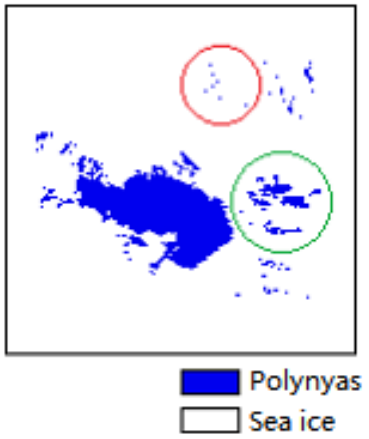

Figure 4. Threshold method based on sea ice density

5. Conclusion

This paper proposes a new method for detecting the distribution of polynyas based on AMSR2 19GHz data. First, the 19GHz vertical and horizontal brightness temperature data are processed to obtain the polarization difference. Secondly, the maximum entropy method is used to process the polarization difference data to obtain the optimal threshold for the identification of the polynyas, so as to obtain the results of the polynyas on October 15, 2017. Finally, the method proposed in this paper is comparing with the sea ice density threshold method. The results show that the distribution results of polynyas obtained by the two are basically the same, and its accuracy is higher than that of the sea ice density threshold method.

References

[1] Smith S; Muench R; Pease C H. Polynyas and leads: An overview of physical processes and environment, Journal of Geophysical Research, 1990; Volume 95, pp. 9461-9479.

[2] Maqueda M A M; Willott A J, Biggs N R T. Polynya dynamics: A review of observations and modeling, Review of Geophysics, 2004; Volume 42(1), RG1004.

[3] Gao. G. P.; Dong. Z. Q. Research progress on the formation mechanism of polynyas in the Weddell Sea, Antarctica, Periodical of Ocean University of China, 2004; Volume 34(1), pp. 1-6.

[4] Alam A; Curry J. Lead-induced atmospheric circulations, Journal of Geophysical Research, 1995; Volume 100, pp. 4643-4651.

[5] Liang. M. Y.; Shi. J. X. Variations in coastal polynyas in the Alaskan Chukchi sea and major influencing factors, Chinese Journal of Polar Research, 2015; Volume 27(4), pp. 379-391.

[6] Fu. H. L.; Kang J. J.; Li X.; et al. study of the varibility of polynyas in the arctic based on the AMSR-E sea ice concentration, Chinese Journal of Polar Research, 2014; Volume 26(2), pp. 243-253.

[7] Massom R A; Harris P T; Michael K J; et al. The distribution and formative processes of latent-heat polynyas in East Antarctica, Annals of Glaciology, 2017; Volume 27, pp. 420-426.

[8] Stringer W J; Groves J E. Location and areal extent of polynyas in the Bering and Chukchi Seas, Arctic, 1991; Volume 44(5), pp. 164-171.

[9] Ciappa A; Pietranera L, Budillon G. Observations of the Terra Nova Bay (Antarctica) polynya by MODIS ice surface temperature imagery from 2005 to 2010, Remote sensing of environment; Volume 119, pp. 158-172.

[10] Haid V, Timmermann R. Simulated heat flux and sea ice production at coastal polynyas in the southwestern Weddell Sea, Journal of Geophysical Research, 2013; Volume 118, pp. 2640-2652.

[11] Spreen G; Kaleschke L; Heygster G. Sea ice remote sensing using AMSR-E 89-GHz channels, Journal of Geophysical Research Oceans, 2008; Volume 113(C2).

[12] Wiebe H; Heygster G; Markus T. Comparison of the ASI Ice Concentration Algorithm With Landsat-7 ETM+ and SAR Imagery, IEEE Transactions on Geoscience and Remote Sensing, 2009; Volume 47(9), pp. 3008-3015.